Electronic Supplementary Material (ESI) for ChemComm.

Spin Crossover Modulation in a Coordination Polymer with the Redox-active bis-pyridyltetrathiafulvalene (py_2TTF) Ligand

Lisa Zappe,[a] Sophie Schönfeld,[a] Gerald Hörner,[a] Katrina A. Zenere,[b] Chanel F. Leong,[b] Cameron J. Kepert,[b] Deanna M. D'Alessandro,[b] Birgit Weber*[a] and Suzanne M. Neville*[c]

[a] Department of Chemistry, University of Bayreuth, Universitätsstraße 30, 95448 Bayreuth, Germany. weber@uni-bayreuth.de.

[b] School of Chemistry, The University of Sydney, Sydney, New South Wales, 2006, Australia.

[c] School of Chemistry, University of New South Wales, Sydney, NSW 2052, Australia

Contents

S1: Experimental

Synthesis of $[FeL_a(py_2TTF)]_n$: A suspension of $[FeL_a(MeOH)_2]$ (0.21 g, 0.47 mmol) and py_2TTF (0.18 g, 0.50 mmol) in ethanol (20 mL) was heated to reflux for 3 h. After cooling and left to stand to room temperature for 2 days, the red crystalline solid was filtered off. The precipitate (comprised of both polycrystalline powder and single crystals) was three times washed with ethanol (3 mL) and dried in vacuo to give of **$[FeL_a(py_2TTF)]_n$** (yield 0.19 g, 52.58 %). Elemental analysis calcd (%) for $C_{35}H_{30}FeN_4O_4S_4$ (754.05 g mol^{-1}) C 55.70, H 4.01, N 7.42, S 16.99; found: C 54.89, H 3.83, N 7.61, S 17.50. MS (DEI-(+), 70 eV): m/z (%): 358 (100) $[py_2TTF]$, 382 (56) $[[FeL_a]]$, 179 (57) $[C_8H_5NS_2^{2\cdot}]$, 103 (97) $[C_3H_3S_2^{\cdot}]$, 76 (25) $[C_6H_4^{2\cdot}]$

Single crystal diffraction. Single-crystal data were collected at 100 K on MX-1 at the Australian Synchrotron (λ = 0.71073 Å).[1] Data were collected using the Blue Ice software.[2] Initial data processing was carried out using the XDS package.[3] Structural solution was completed with SHELXT[4] and refined using SHELXL[5] within the OLEX2 user interface.[6] All non-disordered atoms were refined anisotropically and hydrogen atoms were fixed using the riding model. We note that the crystal was quench-cooled to 100 K for data collection due to the operational condition constraints at the Australian Synchrotron – quench-cooling is known to potentially lead to HS state trapping. We further note that magnetic susceptibility measurement data shows that the crystal is mid spin-state transition at 100 K (~15% LS of a total of 25% below) so we would only expect a small change in Fe-N bond lengths between HS and LS at this temperature.
The entire equatorial ligand (**L_a2**) was modelled as two positionally disordered components (**A** and **B**). The **Fe2** site was also modelled as two parts as the thermal ellipsoid was substantially elongated within the **L_a2** plane. The disordered parts were modelled isotropically and the thermal parameters of equivalent components were fixed to be equivalent (EADP) and their occupancies were refined to a total of 1 (FVAR) with a 48:52 ratio of the two parts observed.
The solvent was unable to be modelled appropriately, thus was removed from the final model using the BYPASS routine within OLEX2.[6] A summary of the crystallographic and refinement details are located in Table S1 and relevant structural parameters are in Table S2. Crystallographic data has been deposited with the Cambridge Crystallographic Data Centre, CCDC-2004198.

Magnetic susceptibility measurements. Magnetic susceptibility data were collected on a Quantum Design Versalab Measurement System with a vibrating sample magnetometer (VSM) attachment within a small-bore hole cavity. Samples were contained within a polypropylene holder and held within a brass half-tube designed for VSM measurements. Measurements were taken continuously under an applied field of 0.3 T over the temperature range 300 – 50 - 300 K, at a ramp rate of 1 K min^{-1} with no overshoot. The raw data were corrected for the sample holder and diamagnetic contributions.

Mössbauer spectroscopy. ^{57}Fe Mössbauer spectroscopy was recorded in transmission geometry at constant acceleration using a conventional Mössbauer spectrometer with a 50 mCi 57Co(Rh) source. The spectra were fitted using Recoil 1.05 Mössbauer analysis software. Isomer shift values were reported with respect to α-Fe as a reference at room temperature.

DFT calculations. DFT calculations were performed using ORCA2.9.1.[7] Large TZVP basis sets[8] were used throughout. The structures of the truncated axial ligand model **TTFpy** and of the iron(II) complexes **$[L_aFe(py)_2]$** and **$[L_aFe(TTFpy)_2]$** were optimized with the GGA functional BP86.[9] Complexes were optimized in their LS (*S* = 0), IS (*S* = 1) and HS states (*S* = 2). Cartesian coordinates of all optimized structures are compiled in Tables S3-9; structure plots are displayed in Figure S9. Molecular orbital

shapes and energies of the LS and HS species were derived from single-point calculations with the TPPSh hybrid functional.[10] Dispersion contributions were approximated using Grimme's DFT-D3 atom pairwise dispersion corrections.[11] Solvent effects were accounted for in a dielectric continuum approach (COSMO),[12] parameterized for MeCN. Frontier MO diagrams of **TTFpy**, **$[L_aFe(py)_2]$** and **$[L_aFe(TTFpy)_2]$** are given in Figures S10-11.

EPR spectroscopy and EPR spectroelectrochemistry (SEC). Continuous wave X-band EPR measurements were collected on a Bruker EMXnano bench-top spectrometer. Samples were loaded into quartz tubes and spectra were obtained at room temperature. The microwave frequencies used were in the range 9.37-9.99 GHz, and the microwave power was specifically tuned for each sample to prevent signal saturation. The general parameters used were: modulation frequency, 100 kHz; modulation amplitude, 1.0 G; sweep width, 100-200 G; resolution, 1024 points. Spectra were simulated using the WinEPR software and the EasySpin package in MATLAB.

EPR SEC was performed in a hand-made three electrode setup in a glass pipette with 0.1 M tetrabutylammonium hexafluorophosphate (NBu_4PF_6) in acetonitrile as electrolyte, as reported previously.[13] The prepared pipette was placed in the spectrometer and connected to an eDAQ e-corder 410 potentiostat. The potentials were ramped in 0.05 V increments as corresponding spectral changes were recorded continuously for minimum 1 minute to allow an equilibration of the sample. A reducing potential of -0.01 V was applied after the measurement was finished, to reduce the oxidized sample slowly.

Cyclic Voltammetry. DC Cyclic Voltammetry (CV) was performed using a BASi Epsilon Electrochemical Analyser potentiostat in a three-electrode cell setup. The electrodes were a glassy carbon working electrode, a Pt wire auxiliary electrode and an Ag/Ag^+ quasi-reference electrode. The working electrode was prepared by polishing the active surface with fine alumina on microfibre cloth. The Pt and Ag wires were both rinsed with concentrated HNO_3, de-ionised water and acetone. The Ag wire was polished with fine abrasive paper. The electrolyte which was a solution of 0.1 M tetrabutylammonium hexafluorophosphate (NBu_4PF_6) in acetonitrile was degassed under a flow of high purity Ar for a minimum of 5 min prior to measurements. Prior to the measurement, a full potential sweep was performed to detect any impurities in the cell. The solid sample was dip coated onto the glassy carbon working electrode via mechanical immobilisation, whereby the working electrode was dipped into a slurry of the powdered sample in solvent. The working electrode was lowered slowly into the electrolyte to avoid a loss of contact between the sample and the electrode surface. The sample at the surface of the working electrode was refreshed prior to each potential sweep. Experiments were performed by measuring the current as a function of the potential with a scan rate of 100 mVs^{-1}. Ferrocene was added as an internal reference after the conclusion of each experiment, and potentials were referenced to the ferrocene/ferrocenium (Fc/Fc^+) couple. It is important to note that for similar Schiff-base compounds reported in the literature, the potentials are commonly referenced to the Standard Hydrogen Electrode (SHE); for example, the potential for the Fc/Fc^+ couple is given as 0.785 V versus the SHE in acetonitrile solvent containing NBu_4ClO_4 electrolyte.[14-15] In the present work, of particular interest were the potentials for oxidation of the TTF units. In the literature, and in our own previous work, these are typically reported relative to the Fc/Fc^+ couple; for this reason, the experimental electrochemical data (Figures S2 and S3) is reported relative to this internal standard. Square wave voltammetry was measured as described with a speed of 100 mVs^{-1} and settings to 40 mV at 19 Hz.

Diffuse Reflectance UV-VIS-NIR Spectroscopy. Diffuse reflectance UV/VIS/NIR spectroscopy was performed on a CARY 5000 Spectrophotometer equipped with a Harrick Praying Mantis attachment. The solid, powdered samples were prepared on a dry $BaSO_4$ matrix and measured using the Praying

Mantis attachment. Spectra were collected in the range from 5000 to 40000 cm^{-1} at a scan rate of 6000 cm^{-1}/min.

UV-VIS-NIR Spectroelectrochemistry. Solid state UV/VIS/NIR SEC was performed in a custom-made Teflon SEC cell comprised of two side arms separately accommodating a Pt wire auxiliary electrode and an Ag/Ag^{+} wire quasi reference electrode, as reported previously.[16] The Pt and Ag wires connect to a central compartment that harbours the electrolyte and a transparent Indium-Tin-Oxide (ITO)-coated quartz working electrode which formed a seal over the top of the compartment. The sample was immobilized onto the conductive ITO side of the working electrode by a strip of Teflon tape and the circuit was completed using copper tape. This slide was inverted over the central compartment to enable contact between the sample and the electrolyte and was finally fixed with adhesive tape to avoid movement. Spectra were collected on a CARY 5000 Spectrophotometer equipped with a Harrick Omni-Diff Probe attachment which was positioned over the sample as viewed through the transparent working electrode. A baseline correction was performed on exposed Teflon Tape. Continuous collections were made in the range 5000-25000 cm^{-1} at a scan rate of 6000 cm^{-1}/min. Potential was applied with an eDAQ e-corder 410 potentiostat in 0.05 V increments and the corresponding spectral changes were recorded for a minimum of 1 minute to allow for equilibration of the sample. An electrolyte of 0.1 M tetrabutylammonium hexafluorophosphate (NBu_4PF_6) in acetonitrile was used.

Powder X-ray diffraction. Powder diffraction was performed with a PANalytical X'Pert PRO Diffractometer, employing Cu-Ka (λ = 1.5406 Å) radiation and equipped with a solid state PIXcel detector. Diffraction patterns of dry samples were collected on a spinning goniometer in flame sealed glass capillaries over the range 2θ = 2 – 40°.

S2: Single crystal X-ray diffraction

Table S1. Crystal data for **$[FeL_a(py_2TTF)]_n$** at 100 K.

Parameter	Value
Empirical formula*	$C_{68}H_{56}Fe_2N_8O_8S_8$
Formula weight/ g mol^{-1}	1478.47
T /K	100
Crystal system	Triclinic
Space group	*P*-1
a/Å	13.268(3)
b/Å	15.980(3)
c/Å	18.693(4)
α/°	67.82(3)
β/°	76.64(3)
γ/°	81.97(3)
Volume/Å^3	3564.5(15)
Z	2
ρ_{calc} g/cm^3	1.3774
μ/mm^{-1}	0.700
Data/restraints/parameters	16666 / 142 / 803
Goodness-of-fit on F^2	1.1048
Final R indexes [I>=2σ (I)]	R_1 = 0.1160, wR_2 = 0.3173
Final R indexes [all data]	R_1 = 0.1567, wR_2 = 0.3753

*The solvent has been omitted from the model (SQUEEZE) and formula.

Table S2. Summary of selected structural parameters for **$[FeL_a(py_2TTF)]_n$** at 100 K.

Selected parameters	Fe1-L1-L_a1	Fe2-L2-L_a2 (part A)	Fe2-L2-L_a2 (part B)
$d_{<Fe-X>}$/Å	2.127(2)	2.137(5)	2.121(6)
$d_{<Fe-N(Py)>}$/Å	2.279(2)	2.271(2)	2.256(4)
$d_{<Fe-LaX>}$/Å	2.051(2)	2.071(2)	2.052(7)
O-Fe-O	112.7(2)	112.7(4)	115.1(4)
TTF C=C	1.348(10)	1.341(11)	

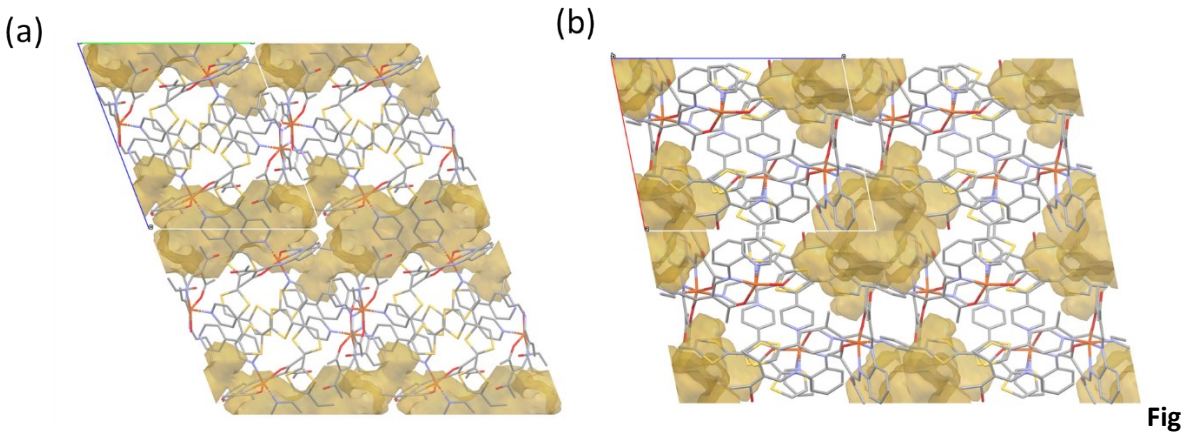

Figure S1: Crystal packing diagram of **[FeL$_a$(py$_2$TTF)]$_n$** showing the vdW surface of the 1-D channels. Viewed along the (a) *a*-axis and (b) *b*-axis. The channels are continuous along the *b*-direction but do not link together. Only the 'B' disordered component is shown for clarity.

S3. Cyclic voltammetry

Solid-state CV

The compound **[FeL$_a$(py$_2$TTF)]$_n$** shows four processes (Figure S2a). The first two processes at $E_{1/2}$ of 0.17 V versus Fc^+/Fc and $E_{½}$ of 0.54 V versus Fc^+/Fc are quasi reversible and were assigned to be the first and second oxidation of the TTF core. The third and fourth process at 0.87 and 0.99 V versus Fc/Fc^+ showed no reversibility and were assigned to the first and second oxidation of the equatorial ligand L_a. The presence of a $Fe^{II/III}$ process in this region was discounted, as previous literature reports for Schiff-base Fe^{II} polymers show that these processes occur at very negative potentials.[14-15] A square wave voltammogram, shown in Figure S2b, was performed to confirm the four processes. As in the cyclic voltammogram, the third process can be observed as a small shoulder on the fourth process in the square wave voltammogram, with both processes being very close to one another.

Furthermore, the reversibility of the first and second processes was measured by cycling the CV three times. The first process was characterised by cycling the potential from -0.45 V to 0.35 V versus Fc/Fc^+ (Figure S3a) and the second process was cycled from -0.45 V to 0.80 V versus Fc/Fc^+ (Figure S3b). The first process was fully reversible during the three redox cycles whereas the second process lost its reversibility with every new cycle.

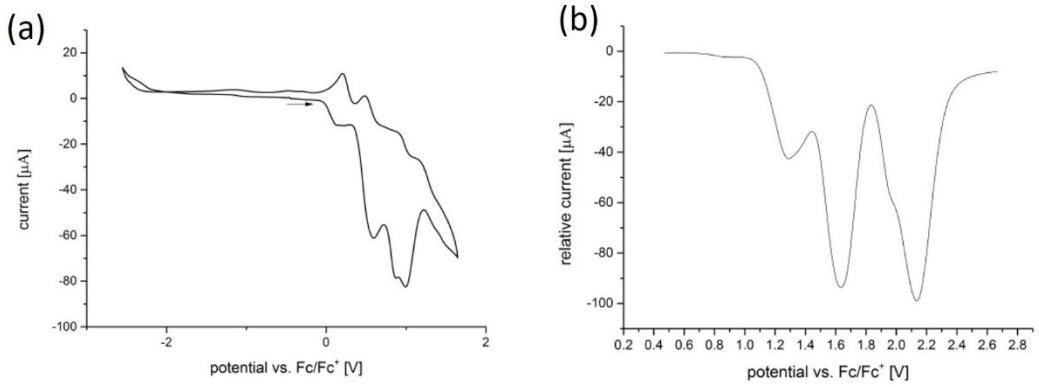

Figure S2. (a) Cyclic voltammogram (the arrow shows the direction of the forward scan) and (b) square wave voltammogram of **[FeL$_a$(py$_2$TTF)]$_n$**

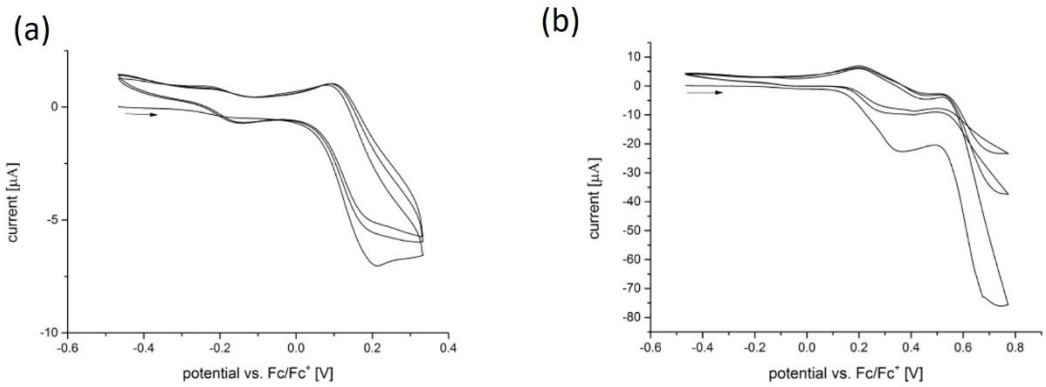

Figure S3. Cyclic voltammogram of **[FeL$_a$(py$_2$TTF)]$_n$** with a potential between (a) -0.40 V and 0.40 V and (b) -0.40 V and 0.80 V. The arrows show the direction of the forward scan.

S4. Electron Paramagnetic Resonance (EPR)

The EPR in a field between 3300 and 3550 G (equivalent to g values in the range 2.12 to 1.96) of dried **[FeL$_a$(py$_2$TTF)]$_n$** showed approximately no signal indicating a neutral TTF species. As the applied potential is increased up to 0.75 V, a signal is observed, indicating the generation of oxidised radical TTF species. This process is reversible up to 0.75 V (Figure S4).

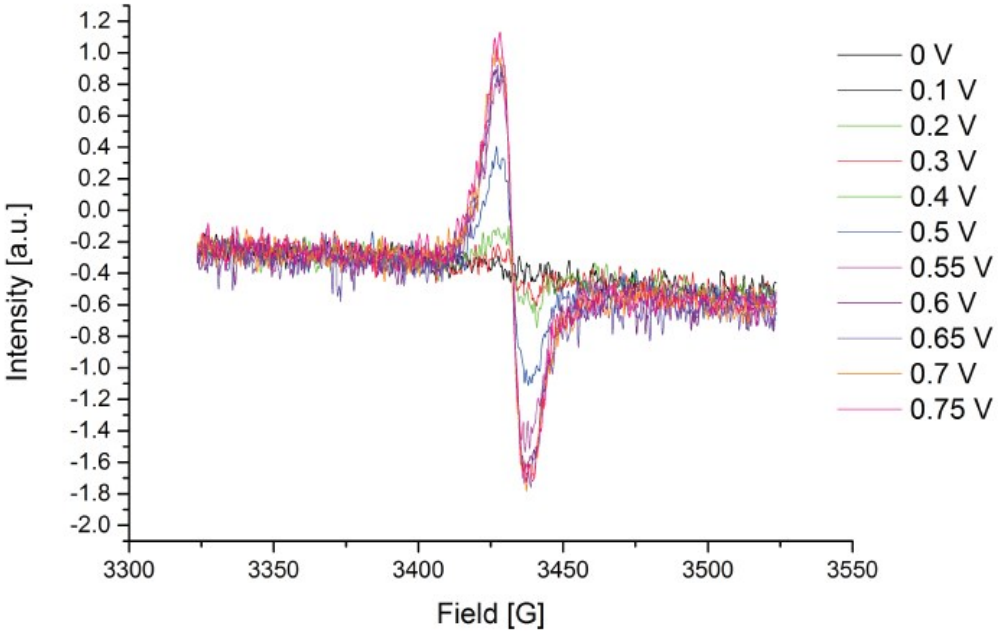

Figure S4. EPR spectrum of **[FeL$_a$(py$_2$TTF)]$_n$** in the region from 3300 to 3550 G over an applied potential range from 0 V to 0.75 V.

S5. Spectroelectrochemistry (SEC)

For further characterisation of **$[FeL_a(py_2TTF)]_n$** in situ solid state UV-VIS-NIR spectroelectrochemistry was performed to determine whether the TTF was oxidised or if other processes take place during oxidation. Figure S5 shows the setup made up by attaching the sample to an indium tin oxide (ITO) glass with a strip of Teflon tape at the top of the cell.[17] The cell was filled with electrolyte, and the counter and reference electrodes were situated at the sides of the cell. The potential was ramped in 0.05 V increments and UV/VIS/NIR spectra were taken during equilibration at each potential. At 0.05 V applied potential, as seen in Figure S6, the red sample leached due to free ligand. The leaching had no further impact on the measurement and stopped after a few seconds. As the applied potential was raised to 0.40 V the colour of the sample turned darker; as it was raised to 0.80 V the sample turned black. As the applied potential was raised to 0.90 V the sample turned dark green and started leaching, leading to the assumption that the compound degraded at that potential.

The UV/VIS/NIR SEC spectrum (Figure S7) of **$[FeL_a(py_2TTF)]_n$** in the region from 5000 to 20000 cm^{-1} (2000 to 500 nm) over an applied potential range from 0 V to 0.90 V is characterised by two absorption bands. The collected data show an absorption at 15000 cm^{-1} (667 nm) appearing, which was assigned to be the oxidised TTF core. The broad absorption band between 6000 and 11000 cm^{-1} (1667 and 909 nm) was tentatively attributed to be the intervalence charge transfer (IVCT) band. The appearance of an IVCT band suggests that as the TTF cores were oxidised, mixed-valence states form.

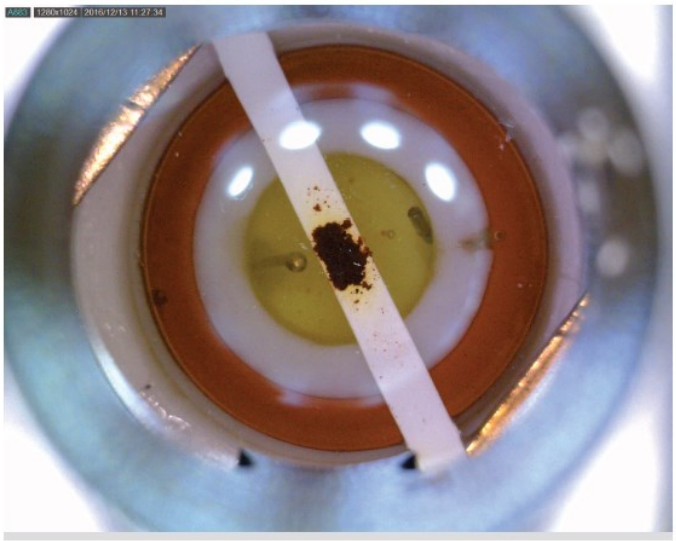

Figure S5: Top view of the cell with the **$[FeL_a(py_2TTF)]_n$** sample attached to the ITO glass in the middle.

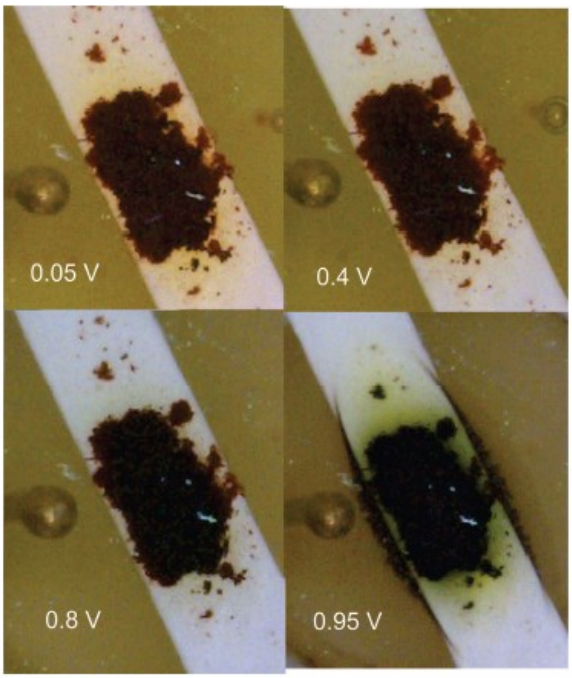

Figure S6: Top view of the cell with a sample of **[FeL$_a$(py$_2$TTF)]$_n$** at 0.05 V, 0.40 V, 0.80 V and the degraded sample at 0.95 V applied potential.

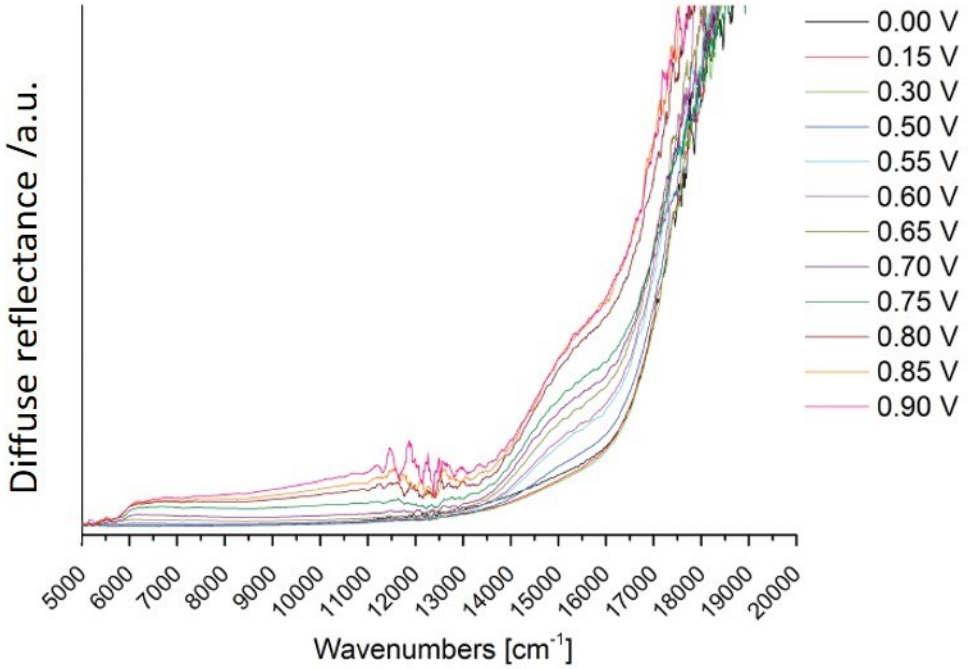

Figure S7: SEC spectrum of **[FeL$_a$(py$_2$TTF)]$_n$** in the region from 5000 to 20000 cm^{-1} (2000 to 500 nm) over an applied potential range from 0 V to 0.90 V.

S6. Powder X-ray diffraction

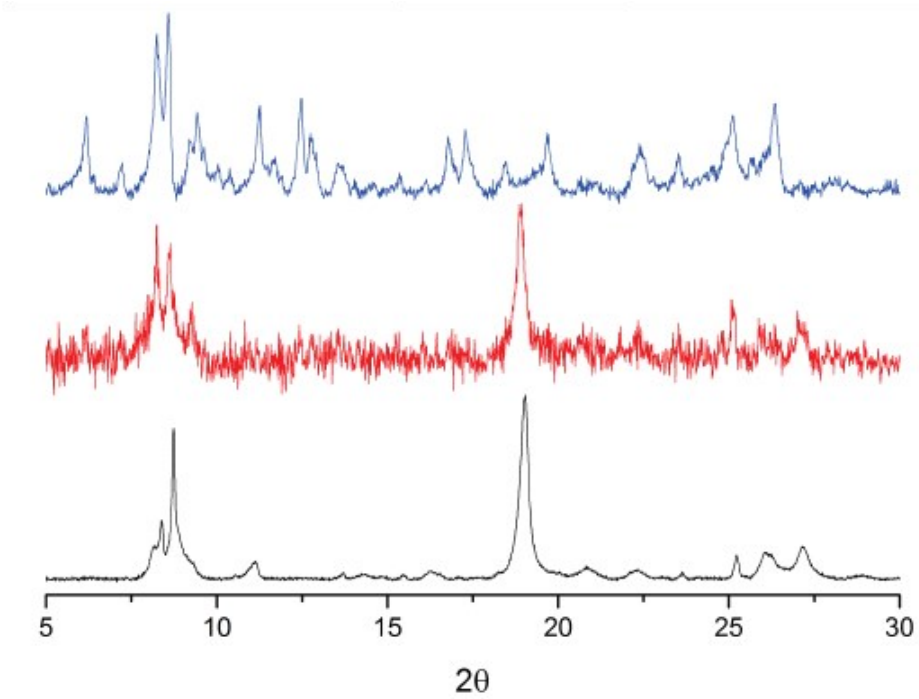

Figure S8: Powder X-ray diffraction comparison of **$[FeL_a(py_2TTF)]_n$** (blue top) and the sample exposed to iodine vapour for 2 days (red middle) and 2 weeks (black bottom).

S8. DFT calculations

Figure S9 shows DFT-optimized structural models for the high spin (*S*=2), low spin (*S*=0) and intermediate spin (*S*=1). The bridging ligand TTF(py)$_2$ is herein approximated either as a truncated TTFpy or simple pyridine ligand, yielding **[L$_a$Fe(TTFpy)$_2$]** and **[L$_a$Fe(py)$_2$]**, respectively. There is no characteristic metrical difference in the inner coordination sphere between both models. It is noticeable from both models that the LS state has a distinctly more planar geometry of the equatorial ligand.

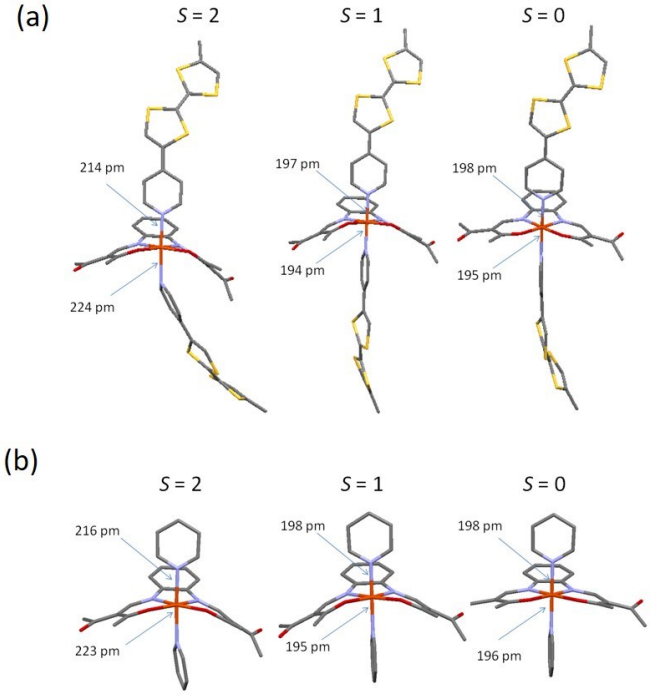

Figure S9: Optimized structures of the *S* = 0, 1 and 2. (a) mononuclear model for TTF-bridged polymer chains, (b) truncated models.

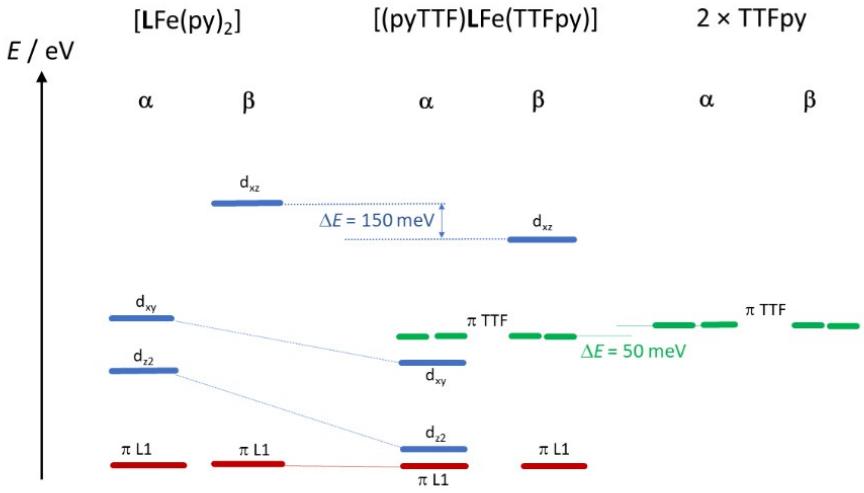

Figure S10. Energy order of the occupied MOs of model complex **[L$_a$Fe(py)$_2$]** (left), of the polymer model **[(pyTTF)L$_a$Fe(TTFpy)]** (middle) and of the truncated ligand **TTFpy** (right); complexes are in the quintet states; metal-centered (blue), L$_a$-centered (red) and TTF-centered (green).

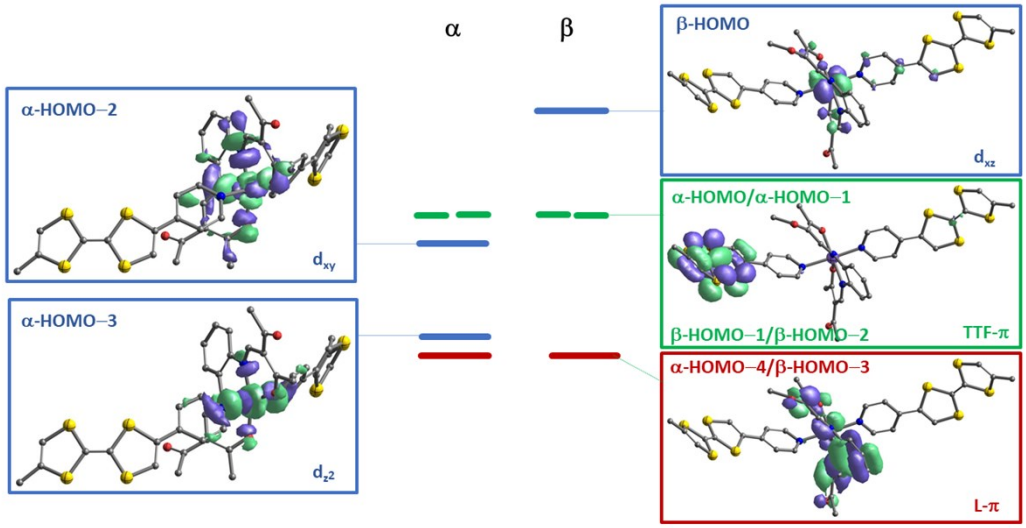

Figure S11. Representations of selected occupied Kohn-Sham frontier MOs of quintet configured **[L_aFe(TTFpy)$_2$]**; color code denotes the dominant character of the MOs.

Table S3. Cartesian coordinates of singlet configured **[L_aFe(py)$_2$]**:

Fe	6.36523	4.09838	7.63525
O	7.87685	5.12982	6.99177
O	6.82225	4.70150	9.42684
N	4.88169	3.07464	8.23239
O	8.69249	6.13253	3.00314
O	3.06067	3.07915	11.84705
N	5.91188	3.46804	5.90438
N	5.22809	5.66936	7.42855
C	4.35390	2.24168	7.22001
C	6.09288	4.62381	10.47845
C	4.34070	3.16437	9.42906
H	3.42253	2.60490	9.63620
C	4.92147	2.45798	5.93598
C	8.19491	5.39445	5.78098
C	6.42798	3.91417	4.77562
H	6.00752	3.51672	3.84978
C	7.48828	4.86079	4.63946
C	4.82427	3.95485	10.51515
C	3.37062	1.25378	7.39213
H	2.95062	1.06080	8.37954
C	3.92213	3.96872	11.68646
C	2.94404	0.49658	6.29832
H	2.18507	-0.27502	6.44034
C	4.49288	1.68018	4.84713
H	4.93814	1.81193	3.86063
C	7.85310	5.24903	3.26610
C	3.50404	0.70979	5.02786
H	3.18169	0.10535	4.17838
C	9.39887	6.29297	5.64470
H	10.14557	5.86001	4.96349
H	9.10786	7.25673	5.20104
H	9.82855	6.45172	6.64328
C	6.74326	5.21884	11.70893
H	6.50111	4.66439	12.62366
H	7.83097	5.22049	11.55434
H	6.42033	6.26303	11.84948
C	3.94194	5.11864	12.68135
H	4.32078	6.05431	12.25241
H	2.91499	5.26228	13.04451
H	4.56944	4.86026	13.55000
C	7.17047	4.54775	2.09008
H	7.30738	3.45522	2.13223
H	6.08645	4.74730	2.08297
H	7.60904	4.93290	1.16125
C	3.57297	7.96954	7.26188
C	4.88379	8.03083	7.79042

H	5.30558	8.97149	8.14441
H	6.66921	6.90521	8.26791
C	5.66027	6.88764	7.86113
C	3.98173	5.60586	6.89551
C	3.14316	6.70746	6.80036
H	2.14615	6.56482	6.38160
H	3.65603	4.62792	6.54691
N	7.53541	2.52517	7.88811
C	8.39779	2.12043	6.91768
C	7.47755	1.78536	9.02133
H	6.77702	2.12729	9.78156
C	8.24555	0.64461	9.21831
H	8.12355	0.09029	10.15007
H	8.42812	2.73432	6.01875
C	9.19975	0.99809	7.04289
H	9.87552	0.74432	6.22678
C	9.13526	0.20882	8.21354
H	9.78551	-0.55353	8.82517
H	3.07011	8.70169	7.23945

Table S4. Cartesian coordinates of triplet configured **[L_aFe(py)$_2$]**:

Fe	6.353075	4.091314	7.649457
O	7.865531	5.120551	7.006184
O	6.803538	4.698546	9.440406
N	4.867829	3.070585	8.245282
O	8.679402	6.129047	3.018503
O	3.060984	3.041129	11.866741
N	5.901980	3.460183	5.918908
N	5.224212	5.677252	7.428176
C	4.337801	2.239414	7.232157
C	6.079563	4.614072	10.494977
C	4.329696	3.152228	9.444162
H	3.413280	2.590032	9.651296
C	4.908667	2.453128	5.948882
C	8.184678	5.385670	5.795956
C	6.417340	3.906027	4.789413
H	5.995434	3.510274	3.863504
C	7.478430	4.852454	4.653573
C	4.814979	3.936465	10.534773
C	3.350569	1.254844	7.401990
H	2.927259	1.063329	8.388279
C	3.919699	3.935096	11.710309
C	2.923091	0.498616	6.307634
H	2.160811	-0.270004	6.448507
C	4.479270	1.676122	4.859606
H	4.927238	1.805644	3.873983
C	7.841811	5.242934	3.281584
C	3.486475	0.709178	5.038237
H	3.163634	0.105705	4.188183
C	9.389450	6.283757	5.660257
H	10.135225	5.852491	4.976931
H	9.099111	7.249442	5.220165
H	9.820469	6.439167	6.658847
C	6.732684	5.209074	11.724594
H	6.503534	4.646675	12.637965
H	7.819136	5.222527	11.561885
H	6.400519	6.249028	11.874608
C	3.941941	5.071809	12.720715
H	4.310644	6.015911	12.301639
H	2.917398	5.203764	13.095095
H	4.578987	4.805870	13.580150
C	7.160402	4.541924	2.104355
H	7.296411	3.449287	2.146639
H	6.076452	4.742090	2.094828
H	7.601024	4.927061	1.176431
C	3.642720	7.985173	7.153073
C	4.918334	8.051795	7.726013
H	5.332057	8.996632	8.080197
H	6.671464	6.887962	8.284070
C	5.675025	6.889304	7.846988
C	3.986713	5.617050	6.871301
C	3.176343	6.738958	6.719333
H	2.191729	6.627142	6.264472
H	3.656421	4.632656	6.545057
N	7.534460	2.519161	7.906474

C	8.405309	2.132844	6.941245
C	7.481732	1.791115	9.049612
H	6.764916	2.129234	9.796574
C	8.287632	0.675121	9.264553
H	8.202290	0.126609	10.203185
H	8.412876	2.737274	6.035326
C	9.241055	1.027337	7.086093
H	9.920287	0.761437	6.275284
C	9.185719	0.278600	8.267075
H	9.826682	-0.593302	8.406080
H	3.029529	8.880932	7.046670

Table S5. Cartesian coordinates of quintet configured **[L_aFe(py)$_2$]**:

Fe	7.23113	4.50288	7.47340
O	8.78256	5.31942	6.50284
O	7.07137	5.14311	9.39535
N	5.42546	3.50318	7.90517
O	9.30106	6.16563	2.42756
O	2.42385	4.84563	10.31734
N	6.78664	3.59237	5.64828
N	5.99038	6.29727	6.94901
C	5.13012	2.48914	6.98101
C	6.00740	5.49797	10.02674
C	4.51315	3.96337	8.72914
H	3.48542	3.58135	8.65313
C	5.87175	2.52971	5.76641
C	8.97653	5.60184	5.26714
C	7.21165	3.99843	4.47079
H	6.73979	3.54574	3.59140
C	8.21419	4.98737	4.21087
C	4.71152	5.00728	9.68848
C	4.20726	1.45502	7.20225
H	3.66572	1.41647	8.14907
C	3.46016	5.53601	10.27046
C	4.01265	0.46630	6.23189
H	3.30122	-0.34130	6.41594
C	5.68455	1.51422	4.81318
H	6.28329	1.50878	3.90101
C	8.44977	5.33365	2.79710
C	4.75178	0.49640	5.03932
H	4.61995	-0.29005	4.29325
C	10.06925	6.61135	5.01343
H	10.84117	6.20015	4.34632
H	9.66733	7.49509	4.49555
H	10.50600	6.90067	5.97911
C	6.25566	6.41086	11.20584
H	5.48914	6.33369	11.98551
H	7.23978	6.16307	11.62886
H	6.29667	7.45826	10.86126
C	3.36936	6.98889	10.71436
H	4.16464	7.61591	10.29518
H	2.39133	7.37168	10.39026
H	3.40855	7.05302	11.81374
C	7.61232	4.65197	1.71345
H	7.76937	3.56083	1.71320
H	6.53524	4.83011	1.86117
H	7.91754	5.05826	0.74100
C	3.84658	8.09056	7.38869
C	5.14355	8.35453	7.88333
H	5.35929	9.26059	8.44926
H	7.16230	7.60835	8.05174
C	6.16218	7.44243	7.64849
C	4.77086	6.07152	6.42548
C	3.68657	6.92250	6.61533
H	2.71900	6.64789	6.19333
H	4.66070	5.14166	5.86457
N	8.34556	2.76877	8.04761
C	9.20040	2.18616	7.17051
C	7.99847	2.05909	9.14310
H	7.30525	2.55403	9.82481
C	8.46222	0.77274	9.39322
H	8.11435	0.25333	10.28734
H	9.46099	2.78685	6.29739
C	9.71794	0.91311	7.34684
H	10.41226	0.51692	6.60550

C	9.33927	0.15189	8.47740
H	9.77455	-0.73149	8.63938
H	3.16516	8.63346	7.52984

Table S6. Cartesian coordinates of singlet configured **[L_aFe(TTFpy)$_2$]**:

Fe	6.365234	4.098383	7.635252
S	1.827422	11.660832	7.608337
S	1.241561	9.107148	6.170088
O	7.876855	5.129821	6.991772
O	6.822247	4.701502	9.426838
N	4.881692	3.074636	8.232387
O	8.692486	6.132533	3.003141
O	3.060674	3.079151	11.847050
N	5.911881	3.468041	5.904380
N	5.228093	5.669365	7.428553
C	4.353896	2.241681	7.220013
C	6.092882	4.623813	10.478447
C	4.340703	3.164372	9.429056
H	3.422535	2.604902	9.636201
C	4.921467	2.457977	5.935980
C	8.194907	5.394453	5.780984
C	6.427985	3.914165	4.775618
H	6.007517	3.516716	3.849779
C	7.488280	4.860792	4.639463
C	2.952301	10.330260	7.832496
H	3.819441	10.528329	8.461656
C	4.824270	3.954853	10.515153
C	0.594885	10.655831	6.783158
C	3.370619	1.253781	7.392130
H	2.950617	1.060805	8.379539
C	3.922126	3.968719	11.686462
C	2.944042	0.496585	6.298324
H	2.185066	-0.275016	6.440341
C	4.492880	1.680182	4.847135
H	4.938139	1.811931	3.860628
C	7.853103	5.249027	3.266098
C	3.504044	0.709795	5.027863
H	3.181693	0.105346	4.178382
C	2.719803	9.150113	7.205029
C	9.398867	6.292967	5.644703
H	10.145571	5.860008	4.963493
H	9.107858	7.256735	5.201035
H	9.828547	6.451721	6.643276
C	6.743258	5.218841	11.708927
H	6.501109	4.664386	12.623662
H	7.830966	5.220492	11.554343
H	6.420330	6.263031	11.849482
C	3.941936	5.118635	12.681351
H	4.320779	6.054310	12.252407
H	2.914988	5.262279	13.044511
H	4.569438	4.860260	13.549999
C	7.170475	4.547752	2.090082
H	7.307382	3.455222	2.132226
H	6.086452	4.747304	2.082974
H	7.609040	4.932905	1.161255
C	-0.702465	11.030336	6.641890
S	-1.932431	10.009111	5.835613
C	-3.307716	10.957402	6.434603
S	-1.350311	12.584632	7.243848
C	3.572974	7.969542	7.261879
C	4.883789	8.030832	7.790420
H	5.305579	8.971490	8.144410
H	6.669214	6.905208	8.267914
C	5.660267	6.887635	7.861130
C	3.981727	5.605862	6.895507
C	3.143156	6.707459	6.800364
H	2.146151	6.564820	6.381600
H	3.656027	4.627917	6.546909
N	7.535408	2.525171	7.888108
C	8.397785	2.120425	6.917685
C	7.477554	1.785358	9.021331
H	6.777022	2.127294	9.781563
C	8.245553	0.644609	9.218305
H	8.123548	0.090293	10.150068
H	8.428120	2.734315	6.018746

C	9.199749	0.998087	7.042885
H	9.875524	0.744319	6.226781
C	9.135263	0.208819	8.213536
C	9.947372	-0.994077	8.364283
C	10.633618	-1.613980	7.372249
H	10.651666	-1.276884	6.336655
S	10.139996	-1.717963	10.005525
S	11.599701	-3.029993	7.749043
C	10.954385	-3.194521	9.412458
C	11.064346	-4.331623	10.145630
S	10.394660	-4.498048	11.797695
S	11.887034	-5.806648	9.558416
C	11.233808	-6.876631	10.840803
C	10.568049	-6.264073	11.835436
H	10.151579	-6.779638	12.700677
C	-3.073498	12.118571	7.070461
H	-4.302624	10.567391	6.221141
C	-4.100362	13.071996	7.599818
H	-5.106003	12.696634	7.363292
H	-3.983205	14.070207	7.146977
H	-4.012563	13.187263	8.692461
C	11.519084	-8.342780	10.726084
H	11.056848	-8.769544	9.821435
H	11.118700	-8.865030	11.606404
H	12.603972	-8.530538	10.668832

Table S7. Cartesian coordinates of triplet configured **[L_aFe(TTFpy)$_2$]**:

Fe	7.231129	4.502880	7.473399
S	1.289376	10.918442	8.872244
S	1.192022	8.801697	6.761847
O	8.782557	5.319416	6.502841
O	7.071367	5.143105	9.395350
N	5.425460	3.503182	7.905171
O	9.301061	6.165631	2.427559
O	2.423854	4.845625	10.317344
N	6.786643	3.592370	5.648277
N	5.990380	6.297275	6.949010
C	5.130120	2.489138	6.981014
C	6.007404	5.497974	10.026742
C	4.513148	3.963374	8.729136
H	3.485415	3.581351	8.653129
C	5.871750	2.529707	5.766409
C	8.976532	5.601836	5.267142
C	7.211653	3.998425	4.470792
H	6.739795	3.545743	3.591402
C	8.214186	4.987367	4.210866
C	2.730746	9.951915	8.630779
H	3.589442	10.200441	9.252623
C	4.711524	5.007284	9.688477
C	0.257696	9.881946	7.836450
C	4.207261	1.455020	7.202247
H	3.665718	1.416469	8.149068
C	3.460165	5.536007	10.270460
C	4.012652	0.466295	6.231890
H	3.301219	-0.341303	6.415942
C	5.684549	1.514218	4.813180
H	6.283295	1.508779	3.901010
C	8.449768	5.333647	2.797104
C	4.751783	0.496399	5.039318
H	4.619945	-0.290049	4.293246
C	2.726941	8.974440	7.691189
C	10.069248	6.611350	5.013426
H	10.841168	6.200145	4.346318
H	9.667332	7.495091	4.495547
H	10.505995	6.900667	5.979107
C	6.255658	6.410861	11.205835
H	5.489136	6.333692	11.985512
H	7.239777	6.163072	11.628857
H	6.296675	7.458265	10.861261
C	3.369360	6.988887	10.714363
H	4.164640	7.615910	10.295184
H	2.391329	7.371682	10.390262
H	3.408552	7.053019	11.813738
C	7.612321	4.651973	1.713446
H	7.769370	3.560830	1.713199

H	6.535236	4.830111	1.861174
H	7.917540	5.058263	0.740996
C	-1.099253	9.909764	7.867980
S	-2.119874	8.848688	6.849968
C	-3.610254	9.190056	7.750539
S	-2.039114	11.001559	8.926406
C	3.846577	8.090559	7.388693
C	5.143551	8.354531	7.883328
H	5.359287	9.260586	8.449256
H	7.162302	7.608352	8.051738
C	6.162179	7.442433	7.648486
C	4.770862	6.071518	6.425476
C	3.686574	6.922503	6.615327
H	2.718999	6.647886	6.193326
H	4.660700	5.141659	5.864569
N	8.345559	2.768773	8.047607
C	9.200395	2.186156	7.170510
C	7.998466	2.059086	9.143103
H	7.305251	2.554025	9.824806
C	8.462215	0.772744	9.393219
H	8.114352	0.253331	10.287337
H	9.460991	2.786845	6.297389
C	9.717943	0.913108	7.346837
H	10.412257	0.516922	6.605503
C	9.339270	0.151894	8.477396
C	9.832067	-1.206715	8.674960
C	10.477122	-1.957715	7.747632
H	10.701711	-1.622159	6.736282
S	9.642075	-1.978646	10.294934
S	11.035646	-3.564990	8.178537
C	10.156993	-3.597248	9.739500
C	9.899915	-4.739463	10.426967
S	8.999501	-4.767896	11.974313
S	10.419987	-6.358862	9.875280
C	9.370684	-7.261883	11.015126
C	8.744306	-6.524169	11.948484
H	8.110668	-6.939745	12.732211
C	-3.600932	10.152350	8.688998
H	-4.494755	8.618794	7.469656
C	-4.765948	10.610710	9.511475
H	-5.664902	10.051078	9.217759
H	-4.956836	11.686441	9.361099
H	-4.584068	10.449364	10.586731
C	9.316301	-8.751728	10.867660
H	8.881416	-9.041283	9.897262
H	8.700758	-9.178835	11.671824
H	10.325548	-9.191536	10.925951

Table S8. Cartesian coordinates of quintet configured **[L_aFe(TTFpy)$_2$]**:

Fe	7.231129	4.502880	7.473399
S	1.289376	10.918442	8.872244
S	1.192022	8.801697	6.761847
O	8.782557	5.319416	6.502841
O	7.071367	5.143105	9.395350
N	5.425460	3.503182	7.905171
O	9.301061	6.165631	2.427559
O	2.423854	4.845625	10.317344
N	6.786643	3.592370	5.648277
N	5.990380	6.297275	6.949010
C	5.130120	2.489138	6.981014
C	6.007404	5.497974	10.026742
C	4.513148	3.963374	8.729136
H	3.485415	3.581351	8.653129
C	5.871750	2.529707	5.766409
C	8.976532	5.601836	5.267142
C	7.211653	3.998425	4.470792
H	6.739795	3.545743	3.591402
C	8.214186	4.987367	4.210866
C	2.730746	9.951915	8.630779
H	3.589442	10.200441	9.252623
C	4.711524	5.007284	9.688477
C	0.257696	9.881946	7.836450
C	4.207261	1.455020	7.202247
H	3.665718	1.416469	8.149068
C	3.460165	5.536007	10.270460

C	4.012652	0.466295	6.231890
H	3.301219	-0.341303	6.415942
C	5.684549	1.514218	4.813180
H	6.283295	1.508779	3.901010
C	8.449768	5.333647	2.797104
C	4.751783	0.496399	5.039318
H	4.619945	-0.290049	4.293246
C	2.726941	8.974440	7.691189
C	10.069248	6.611350	5.013426
H	10.841168	6.200145	4.346318
H	9.667332	7.495091	4.495547
H	10.505995	6.900667	5.979107
C	6.255658	6.410861	11.205835
H	5.489136	6.333692	11.985512
H	7.239777	6.163072	11.628857
H	6.296675	7.458265	10.861261
C	3.369360	6.988887	10.714363
H	4.164640	7.615910	10.295184
H	2.391329	7.371682	10.390262
H	3.408552	7.053019	11.813738
C	7.612321	4.651973	1.713446
H	7.769370	3.560830	1.713199
H	6.535236	4.830111	1.861174
H	7.917540	5.058263	0.740996
C	-1.099253	9.909764	7.867980
S	-2.119874	8.848688	6.849968
C	-3.610254	9.190056	7.750539
S	-2.039114	11.001559	8.926406
C	3.846577	8.090559	7.388693
C	5.143551	8.354531	7.883328
H	5.359287	9.260586	8.449256
H	7.162302	7.608352	8.051738
C	6.162179	7.442433	7.648486
C	4.770862	6.071518	6.425476
C	3.686574	6.922503	6.615327
H	2.718999	6.647886	6.193326
H	4.660700	5.141659	5.864569
N	8.345559	2.768773	8.047607
C	9.200395	2.186156	7.170510
C	7.998466	2.059086	9.143103
H	7.305251	2.554025	9.824806
C	8.462215	0.772744	9.393219
H	8.114352	0.253331	10.287337
H	9.460991	2.786845	6.297389
C	9.717943	0.913108	7.346837
H	10.412257	0.516922	6.605503
C	9.339270	0.151894	8.477396
C	9.832067	-1.206715	8.674960
C	10.477122	-1.957715	7.747632
H	10.701711	-1.622159	6.736282
S	9.642075	-1.978646	10.294934
S	11.035646	-3.564990	8.178537
C	10.156993	-3.597248	9.739500
C	9.899915	-4.739463	10.426967
S	8.999501	-4.767896	11.974313
S	10.419987	-6.358862	9.875280
C	9.370684	-7.261883	11.015126
C	8.744306	-6.524169	11.948484
H	8.110668	-6.939745	12.732211
C	-3.600932	10.152350	8.688998
H	-4.494755	8.618794	7.469656
C	-4.765948	10.610710	9.511475
H	-5.664902	10.051078	9.217759
H	-4.956836	11.686441	9.361099
H	-4.584068	10.449364	10.586731
C	9.316301	-8.751728	10.867660
H	8.881416	-9.041283	9.897262
H	8.700758	-9.178835	11.671824
H	10.325548	-9.191536	10.925951

Table S9. Cartesian coordinates of singlet configured **TTFpy**:

N	7.498170	2.480626	7.786107
C	8.290872	2.009611	6.797823
C	7.503176	1.785843	8.939289
H	6.862121	2.167594	9.738093

C	8.262096	0.634664	9.151598
H	8.193842	0.117948	10.110315
H	8.286774	2.578503	5.864476
C	9.092004	0.878448	6.912642
H	9.716341	0.578420	6.071522
C	9.088880	0.149403	8.120025
C	9.908928	-1.047003	8.297594
C	10.581962	-1.710015	7.328170
H	10.586471	-1.430536	6.276273
S	10.134716	-1.679853	9.968545
S	11.568802	-3.093738	7.760912
C	10.959389	-3.166455	9.437624
C	11.097196	-4.258474	10.227124
S	10.454522	-4.340024	11.889387
S	11.929612	-5.742904	9.702218
C	11.302916	-6.754683	11.043193
C	10.644430	-6.098356	12.013555
H	10.243061	-6.567484	12.910529
C	11.604818	-8.218433	10.990421
H	11.134371	-8.692964	10.116174
H	11.229753	-8.710225	11.896986
H	12.689178	-8.396580	10.922104

References

1. N. P. Cowieson, D. Arago, M. Clift, D. J. Ericsson, C. Gee, S. J. Harrop, N. Mudie, S. Panjikar, J. R. Price, A. Riboldi-Tunnicliffe, R. Williamson, T. Caradoc-Davides, *J. Synch. Rad.*, 2015, **22**, 187-190.
2. T. M. McPhillips, S. E. McPhillips, H. J. Chiu, A. E. Cohen, A. M. Deacon, P. J Ellis, E. Garman, A. Gonzalez, N. K. Sauter, R. P. Phizackerley, S. M. Soltis, P. Kuhn, P. *J. Synch. Rad.* 2002, **9**, 401.
3. W. J. Kabasch, *J. Appl. Crystallograph.* 1993, **26**, 795.
4. G. M. Sheldrick, *Acta Cryst. A*, 2015, **71**, 3-8.
5. G. M. Sheldrick, *Acta. Cryst. C*, 2015, **C71**, 3-8.
6. O. V. Dolomanov, L. J. Bourhis, R. J. Gildea, J. A. K. Howard and H. Puschmann, *J. Appl. Cryst.*, 2009, **42**, 339-341.
7. F. Neese, *WIREs Comput. Mol. Sci*., 2012, **2**, 73-78.
8. A. Schäfer, H. Horn, R. Ahlrichs, *J. Chem. Phys*., 1992, **97**, 2571**.**
9. A.D. Becke, *Phys. Rev. A*, 1988, **38**, 3098–3100.
10. V. N., Staroverov, G. E. Scuseria, J. Tao, J. P. Perdew, *J. Chem. Phys.*, 2003, **119**, 12129–12137.
11. S. Grimme, J. Antony, S. Ehrlich, H. Krieg, *J. Chem. Phys.*, 2010, **132**, 154104.
12. A. Klamt, G. Schüürmann, *J. Chem. Soc. Perkin Trans.* 1993, **2**, 5, 799-805.
13. C. Hua, J.-Y. Ge, F. Tuna, D. Collison, J.-L. Zuo, D. M. D'Alessandro, *Dalton Trans.*, 2017, **46**, 2998-3007.
14. P. M. Usov, C. Fabian, D. M. D'Alessandro, *Chem. Commun.*, 2012, **48**, 3945-3947.
15. E.-G. Jäger, E. Häussler, M. Rudolph, A. Schneider, *Z. anorg. Allg. Chem.*, 1985, **525**, 67-85.
16. B. Weber, H. Görls, M. Rudolph, E.-G. Jäger, *Inorg. Chim. Acta*, 2002, **337**, 247-265.
17. D. M. D'Alessandro, *Chem. Commun.*, 2016, **52**, 8957-8971.